Response of Geogrid-Reinforced Retaining Wall to Explosive Loading: Part II—Full Scale Tests

R.A. Reid
South Dakota State University; USA

J.G. Collin
Tensar Earth Technologies Inc., USA

ABSTRACT

For over twenty years, reinforced soil walls using concrete or metal facing panels and steel strip reinforcement have been tested and used to protect against explosions. Based on the successful performance of these systems, a research program was conducted in 1993 to determine the response of geogrid reinforced retaining walls to explosions in the retained soil backfill. This paper will report the results of six detonations of 500 pound bombs in the backfill soil of four different geogrid reinforced retaining walls. Each wall was 4.57 m (15 ft) high and 24.38 m (80 ft) wide at their base and reinforced with high density polyethylene uniaxial geogrid. Test data presented includes : 1) soil pressures on the soil/concrete panel interface; 2) panel accelerations; 3) panel displacements; and, 4) strains in the geogrid. This test program quantifies the response of the facing panels and geogrid to pressure wave loading, determined the adequacy of static design criteria for these loading regimes, and documents failure mechanisms.

INTRODUCTION

The construction of military structures to resist airblast and ground shock loads from weapons detonations has traditionally been accomplished through the use of reinforced concrete. This type of construction can be time consuming and expensive, and becomes difficult at remote sites. Unreinforced soil berms have also been constructed around buildings to mitigate blast loads on structures. Their effectiveness in reducing airblast pressures has been previously investigated (Coltharp et al, 1985). However, unreinforced soil berms require large amounts of soil and land area. The soil alone can be of little use for construction of shelters without some means of controlling its geometry. The development of a rapid, inexpensive, simple and effective construction technique for protective shelters at any potential site led to an investigation utilizing reinforced soil. It is proposed that an entire structure could be built with reinforced soil, i.e. effectively closing in an area with a

reinforced soil wall. In this case the facing material would serve as the interior walls, surrounded by the soil backfill.

TESTING PROGRAM

The dynamic response of reinforced soil walls has been evaluated in full scale explosive testing (Richardson, et al, 1977; Eytan and Reid, 1993, Reinforced Earth Company, undated), at small (1:30) scale (Bachus, et al, 1993; Olen, et al, 1994, 1995), and numerically (Bachus et al, 1993). Based on the results of this previous research, three of the primary design variables that effect the design of a reinforced soil wall subjected to explosive loads are: 1) soil properties; 2) reinforcement stiffness; and, 3) weapon size and placement. Due to research program limitations, it was decided only two of these variables would be assessed.

The two design parameters evaluated in this program are the stiffness of the reinforcement and the weapon size and placement. To evaluate these parameters, a wall would be constructed and subjected to enough of a shock load to cause minor deflections to the wall facing. The bomb crater would then be repaired and a second bomb would be placed closer to the wall in order to cause moderate displacements of the wall panels. At this point, the wall would have sustained enough damage to make it unusable for future tests. A duplicate wall would be constructed and the weapon located such that it would cause heavy damage. After these tests, two more walls would be built to the same specifications as the first two, however a stiffer reinforcement material would be used. Tests would then be conducted with weapons at the same standoff distances as used in the first tests.

Based on these tests, data would be collected to: 1) evaluate the load deformation relationships for a given reinforcement subjected to different levels of pressure; 2) compare the load deformation behavior of two similar walls whose only difference is the stiffness of the reinforcement; 3) determine failure mechanisms; and, 4) provide data for validation of a numerical model and small scale tests.

TEST STRUCTURE DIMENSIONS

The selection of the dimensions of the test structure was based primarily on three factors: 1) construction and instrumentation efficiency; 2) observations from previous full-scale tests; and, 3) compatibility with the scaled test programs. To simplify construction and reduce material needs, the size of the structure was kept to a minimum. To reduce instrumentation requirements, the structure was symmetrical about the load source, which was to be buried behind the geometric center of the exposed wall face.

Length of Wall. To determine the length of the test wall, a review of the 1990 full-scale test (Eytan and Reid, 1993), was conducted. This test has extensive data on wall panel deflection from weapon detonations in the soil backfill. This data shows that the most significant

deflections occur within a zone of approximately five panel widths across, centered about the load source. To capture this damage on the planned tests, the wall face should be at least five full panels long.

Height of Wall. The design height (exposed) of the wall was 4.57 m (15 ft), which corresponds to the scaled height of the centrifuge model walls. The face of the wall was 9.14 m (30 ft) long, to ensure it is wider then the crater caused by the weapon detonation. Based on these requirements, each panel should be 1.52 m (5 ft) in height and 1.83 m (6 ft) wide, making the overall wall approximately 24.1 m (79 ft) long at its base and 5.03 m (16.5 ft) high (this includes the 0.46 m (1.5 ft) embedment depth below grade).

The height of the test wall is compatible with previous tests. The 1990 full-scale test used walls approximately 3.75 m (12.3 ft) in height. The 1:30 scale model tests were scaled 4.57 m (15 ft) high walls. Because of the large amount of scaled test data a full-scale test exposed wall height of 4.57 m (15 ft) was selected.

GEOGRID REINFORCEMENT

One of the primary objectives of this research was to establish how the load deformation behavior of a geogrid reinforced soil wall was affected by the geogrid stiffness. It was desired to use geogrid materials equal in as many aspects as possible except for stiffness.

Table 1. Geogrid Properties

Property	Test Method	Value	
		Geogrid A	Geogrid B
Apertures			
Along Roll Length (cm)	Calipers	24.13	24.13
Along Roll Width (cm)	Calipers	1.68	1.68
Thickness (cm)			
Ribs	ASTM D1777-64	0.076	0.14
Junctions		0.254	0.41
Reinforcement (kN/m)			
Long term design			
Creep Limited Strength	ASTM D5262	23.34	38.66
Tensile Modulus	GRI GG1-87	729.7	1458
Dimensions			
Roll Width (m)		1.31	1.31
Roll Weight (N)		169	245

The first constraint that affected the selection of geogrid material was the requirement to

embed the geogrid into the concrete facing panel. Some geogrid materials are made of coated polyester which has been shown to degrade when embedded in portland cement concrete. Because high density polyethylene is resistant to degradation (hydrolysis) in the alkaline environment created by the concrete panel and has excellent stiffness properties under rapid loading, a polyethylene geogrid was sought out. The geogrid materials selected for this test series were geogrid A and B. The two materials are very similar in every respect except for tensile modulus (table 1). The difference in tensile modulus at 2% strain is an order of magnitude. The surface area and opening sizes of the two materials are equal, and the creep limited strength of geogrid B is 1.7 times that of geogrid A. Because these materials are so similar in every respect except for tensile modulus and strength, they were chosen for use in this test. For two equal tests, the performance difference in wall deflection could be potentially attributed to the tensile stiffness of the reinforcement. By using geogrids A and B data would be available to compare to the conclusion drawn from the numerical analysis that reinforcement stiffness, not strength, was a primary factor affecting wall deflection.

TYPE OF FACING PANEL

Numerous facing panel shapes are used in reinforced soil wall construction; cruciform, Georgia Stabilized Earth, full height tilt-up panels, modular block and others. A panel size of 1.52 m (5 ft) in height and 1.83 m (6 ft) in width was selected for the tests. This allowed the full design height and width to be achieved easily and maintain symmetry. A Georgia Stabilized Earth panel shape was selected since a local contractor had experience in their fabrication and could cast them on site within the test schedule.

BACKFILL SOIL

After the wall size was determined, earthwork for construction had to be considered. Because of the amount of soil needed and the limited budget, a local sand was chosen as the backfill material. The sand is referred to as Sky X (Sky ten) sand, a SP-SM sand named after the test range where the tests were to take place. The coefficient of uniformity was C_u = 1.62, D_{50} = 0.24 mm, and ϕ = 33° categorizing this as a uniform fine sand. In place densities and moisture contents are given in table 2.

Table 2. Soil Properties For Each Test

Wall Number	Test Number	Unit Weight (kN/m³)	Moisture Content
1	1	17.09 (108.8 pcf)	11.3 %
2	2 & 3	16.96 (108 pcf)	9.6%
3	4 & 5	16.60 (105.7 pcf)	7.5 %
4	6	16.45 (104.9 pcf)	4.4 %

WALL DESIGN

With selection of the soil, geosynthetic reinforcement, and wall panel type, complete design of the reinforced soil walls proceeded to determine the embedment lengths of the reinforcement. This was initially done using the design procedure outlined in the Federal Highway Report number FHWA-RD-89-043 (Christopher et al, 1990).

Based on this design, the maximum embedment length of the geogrid was 2.52m (8.25 ft), with seven layers of reinforcement. To take advantage of the geogrid manufacturer's expertise in working with their own materials, they were invited to evaluate the design for this problem. Using the geogrid reinforced retaining wall analysis program 'TENSWAL' (version 3.1), a design embedment length of 3.66m (12 ft) was recommended, with nine layers of reinforcement. This embedment length was shortened on the tapered ends of the wall, and two of the layers of reinforcement were not embedded into the wall panels.

The TENSWAL design was more conservative and was selected for use in this test. Due to the unique nature of the test, degree of uncertainty, and lack of data on the response of geogrid reinforced walls to explosive loading, the conservative design was deemed most appropriate. A schematic of the test walls is shown in figure 1.

Figure 1. Schematic of Test Wall

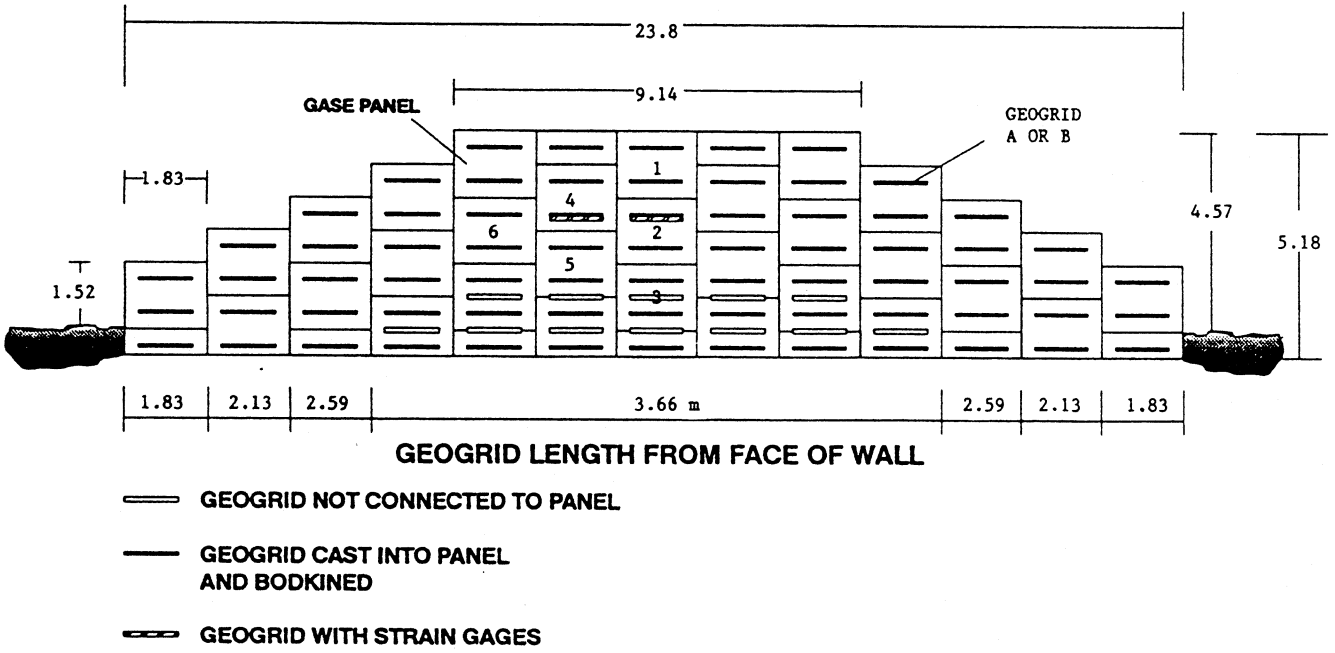

WEAPON SIZE AND PLACEMENT

Many previous explosive tests on hardened reinforced concrete shelters and reinforced soil used 2.22 kN (500 lb) cased general purpose bombs (GP) as an explosive source. These

bombs are referred to as Mark-82 or MK-82 bombs and contain approximately 0.85 kN (192 lb) of high explosive. The 1:30 scale tests also used a scaled explosive designed to model the MK-82. To maintain continuity between tests, this weapon was used in this test series.

As previously established, the distance between the explosive source and the retaining wall has a significant impact on the response of the wall. Based on the review of previous full and small scale test data, a weapon standoff distances of 6.10 m (20 ft), 7.62 m (25 ft) and 9.14 m (30 ft) were selected. The weapon was buried in a vertical orientation such that its center of gravity was 2.29 m (7.5 ft) below the ground surface and centered behind the wall face. This depth corresponded to the horizontal and vertical center of the exposed wall face.

DATA COLLECTION AND INSTRUMENTATION

In order to maximize the benefit of this test to the scientific community, detailed test instrumentation was used to collect data on the response of the wall to conventional weapons detonations. Six accelerometers were attached to the center of the exposed face of the panels numbered one through six (fig. 1) and six soil pressure interface gages were centered at the soil/panel interface centered on the soil side of panels one through six. Twelve strain gages were placed on two pieces of geogrid as shown in figures 1 and 2. Gages S1-S3 and S10-S12 were placed along the centerline of the geogrid layer, while gages S4-S9 were placed three ribs in from the edge of the geogrid layer.Three free field soil pressure gages were located next to strain gages S1-S3. High speed and video cameras were also used to provide a visual record of each test. Details of the gage types, data collection system, installation procedures, and high speed photography are discussed by Reid (1995).

Figure 2. Location of Strain Gages

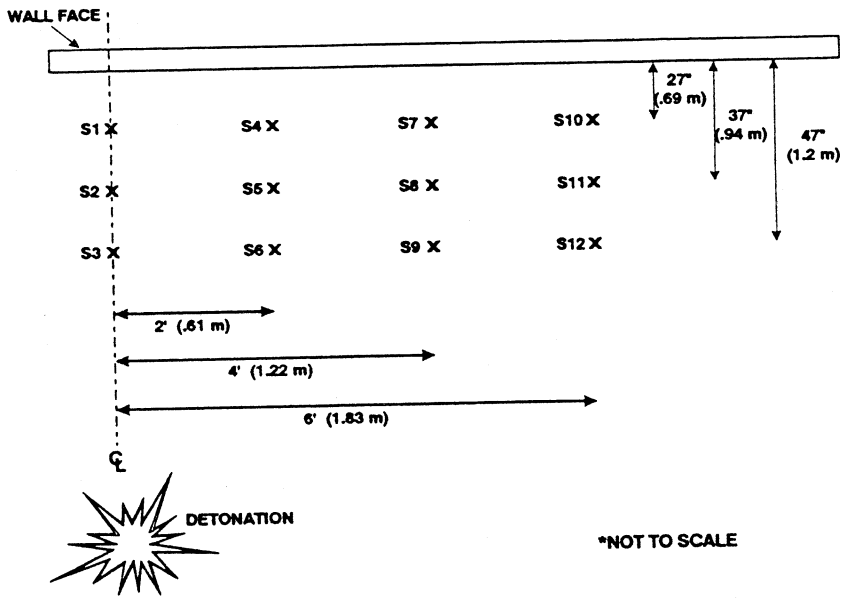

TEST OBSERVATIONS

The walls in tests one and three failed catastrophically after detonation of the weapon. The center portion of both walls completely failed, leaving only the wing walls standing. The walls in tests two, four, and five remained in tact after testing, with varying degrees of displacement. Test six resulted in the failure of only one wall panel, which is identified as panel one in figure 1. The panel moved such that it came to rest face to face with panel two, with panel one hanging by its lower layer of geogrid which still maintained its confining soil. All other panels remained in place. In no instance was geogrid rupture or pullout observed. The final test matrix is shown in table 3.

Table 3. Test Matrix

	Test One	Test Two	Test Three	Test Four	Test Five	Test Six
Geogrid	A	A	A	B	B	B
Weapon Standoff	6.10 m (20 ft)	9.14 m (30 ft)	7.62 m (25 ft)	9.14 m (30 ft)	7.62 m (25 ft)	6.10 m (20 ft)
Result	Total Failure	Wall Survived	Total Failure	Wall Survived	Wall Survived	1 Panel Failed

FAILURE MECHANISMS

Prior to testing, it was anticipated that the initial pressure wave generated by the explosion would have a significant effect on the wall system. This was based on the observations and interpretations of previous research. However, review of the post-test data has identified two separate mechanisms acting on the wall.

Ground Shock Pressure Wave. The ground shock pressure wave propagates through the soil at a measured velocity of 300-335 m/sec (1000 - 1100 ft/sec). Therefore, the main pressure wave arrived at the wall at 20-40 milliseconds (ms) after detonation, depending upon weapon standoff. Data plots of acceleration, pressure, and strain show the arrival and passing of the pressure wave 20-40 ms after detonation, and the time history plots show each of these gages returning to zero and no further readings out to approximately 105 ms when the data recording ceased. The calibrated high speed film of the test, which has a timing light on the film that flashes every ms, did not show any significant movement of the wall facing panels during the passage of the pressure wave. Based on the high speed film, the walls panels did not begin observable motion until at least 200 ms after detonation. At this early stage of data analysis, the authors suggest that this late time effect is due to the dissipation of the gas pressure within the explosive crater.

Parameters of Explosive Waves. After detonation, the explosion cavity is filled with gases in a state of high temperature and pressure which begins to expand. The detonation causes a spherical pressure wave to propagate radially outward. The explosion cavity remains filled

with explosive gases and eventually begins to expand upwards. This results in the formation of the explosive crater. During the formation of the crater, the explosive gases work their way between the soil particles and consequently, a static stress field produced by the gases is released into the soil mass and causes the soil to swell (Henrych, 1979).

Based on the observations from the data collected and the high speed film, both phenomena were observed in this test. All data presented documents the response of the system to the pressure wave only, and not the soil swelling forces caused by cavity expansion. The authors believe that this phenomenon is extremely important and should be considered during the interpretation of the test data, for the pressure wave response may be best described by elastic wave theory, while the explosion cavity expansion causes deformations that may more closely be described by plastic theory.

Toe Failure. Two of the walls failed completely from the soil swell pressure. In each of these cases, the film of the test shows wall panels at the base of the wall (especially panel number three) moving out initially. The panels above the base panels do not move out as much, and therefore have no underlying support. A progressive failure ensues as the upper panels fall vertically.

For the walls that did not fail, the pattern of displacement matched that from the small scale testing. The upper portion of the wall suffered the most lateral displacement, and the base displaced the least. The movement of the top wall panels is not surprising due to the thin layer of confining soil over the geogrid.

RESULTS

Data collection efforts were generally successful with a few exceptions. In test one, none of the strain gages survived construction, so strain data was not obtained. The strain gage installation procedure was modified such that successful measurement of strain did take place in subsequent tests. Due to space constraints, the procedures used for installation of the strain gages will be detailed in a future paper. Also, in test six a major failure of the data collection system led to no data being obtained. Because of the large amount of data collected, and because the detailed test interpretation is still underway, this preliminary presentation will be limited to showing the relationships between pressure and the strain in the respective geogrids, impulse and transmitted stress, and panel velocity and accelerations.

Wavespeed. Each data plot shows both the time of detonation of the explosive and the arrival of the pressure wave group. Since the distance between the gage and detonation was known, as well as the time of arrival, a series of wavespeed measurements existed for each test. These wavespeeds were averaged for each test and the generally consistent results are shown in table 4.

Table 4. Soil Wavespeed for Each Wall

	Test One	Test Two	Test Three	Test Four	Test Five
Wavespeed (m/s)	335 (1099 fps)	316 (1036 fps)	309 (1015 fps)	335 (1100 fps)	316 (1035 fps)
Attenuation Coeff.	3.32	3.56	4.06	3.62	3.66

Pressure. Pressure measurements were not taken at every point where a gage was located. Rather, free field pressure gages were located in the soil mass to get a representative sampling of pressure as a function of time and distance from the detonation. Using those measured free field pressures and the average wavespeed, the attenuation coefficient was determined using the ground shock pressure equation (equation 1) presented by Drake and Little (1983). With wavespeed and attenuation coefficient thus known, the peak free field pressure at any point in the soil mass can then be determined. Pressures were then calculated for each strain gage location and at each wall panel where an accelerometer was installed. The average error between measured free field soil pressures and calculated pressures was 8 percent, with a standard deviation of 8.

$$P = f\, c\, \rho\, \frac{160}{144} \left(\frac{R}{W^{\frac{1}{3}}}\right)^{-n} \qquad (1)$$

where: P = peak pressure in psi
f = ground shock coupling factor
c = seismic velocity of the soil
n = attenuation coefficient
ρ = mass density in (lb-sec/ft^4)
W = charge weight in pounds
R = distance to explosion in feet

Test Data. Test data is presented in table 5. If data was not collected for a specific gage then it is listed as ND for no data. For each test the data is reported for each of the six instrumented panels. Distance refers to the distance between the explosive and the gage. The pressure is calculated by use of the wavespeed, soil mass density, coupling factor, distance from explosive, attenuation coefficient, and charge weight in equation 1. The acceleration represents the peak acceleration measured during the test, and velocity and displacement were calculated by integration of the acceleration vs. time plots. Finally, the soil interface pressure is the measured pressure from the back face of the wall panels. These values are lower than the calculated pressures because of the impedance differential between the soil and the concrete panels. Plots of velocity versus acceleration, interface pressure versus impulse and velocity versus displacement for all tests are shown in figures 3, 4 and 5 respectively. Figure 3 clearly shows the relationship between the increase in panel velocity as a function of acceleration in the range of 0 - 40 g's. The two data points greater than 80

g's may represent a second curve for higher accelerations, however not enough data was collected in this range to fully define this curve. Figure 4 shows the relationship between interface stress (the stress measured at the soil/panel interface) and impulse (area under the interface stress vs time history curve). This interface stress is much less than the free field soil stress due to the difference in the impedance between the soil and the concrete. Finally, the relationship between panel velocity and displacement is shown in figure 5.

Table 5. Test Data

TEST #	PANEL	DISTANCE (m)	PRESSURE (kPa)	ACCELERATION (G's)	VELOCITY (m/sec)	DISPLACEMENT (cm)	SOIL INTERFACE PRESSURE (kPa)	IMPULSE (kPa-sec)
1	1	6.29	410.8	28	0.082	0.048	ND	ND
1	2	6.1	454.6	40	0.079	0.018	28.3	0.101
1	3	6.29	410.8	95	0.079	0.048	41.4	0.142
1	4	6.41	384.8	30	0.027	0.008	16.6	0.052
1	5	6.41	384.8	88	0.042	0.008	271.9	0.626
1	6	7.11	273	22	0.019	0.005	35.9	
2	1	9.27	69.9	28	0.029	0.018	49	0.166
2	2	9.14	73.4	7.1	0.012	0.01	ND	ND
2	3	9.27	69.9	6	0.005	0.003	18.6	0.075
2	4	9.36	67.6	18.2	0.023	0.015	1.6	0.012
2	5	9.36	67.6	13	0.034	0.02	ND	0.092
2	6	9.85	56.3	34		ND	29.7	0.144
3	1	7.77	62	3.1	0.002	0	11.7	0.052
3	2	7.62	67.1	9.6	0.061	0.043	70.4	0.449
3	3	7.77	62	24.3	0.025	0.013	285.7	2.284
3	4	7.87	58.8	8.9	0.021	0.008	114.5	0.384
3	5	7.87	58.8	20.1	0.037	0.033	65.6	0.18
3	6	8.45	44.1	25	0.028	0.015	103.5	0.863
4	1	9.27	66.8	4.4	0.011	0.008	9	0.108
4	2	9.14	70.2	6.9	0.018	0.013	56.6	0.355
4	3	9.27	66.8	15	0.029	0.02	198	0.821
4	4	9.36	64.6	8.4	0.032	0.028	47.6	0.217
4	5	9.36	64.6	35.1	0.061	0.036	47.6	0.165
4	6	9.85	53.7	11.9	0.018	0.01	27.6	0.087
5	1	7.77	112.1	15	0.041	0.028	13.8	0.199
5	2	7.62	120.5	9.3	0.024	0.015	33.1	0.077
5	3	7.77	112.1	31.4	0.043	0.033	315.3	2.336
5	4	7.87	107	10	0.038	0.033	15.9	0.081
5	5	7.87	107	ND	0.075	0.046	62.1	0.207
5	6	8.45	82.5	12.1	0.023	0.018	32.4	0.097

Figure 3. Plot of Wall Panel Velocity vs. Wall Panel Acceleration

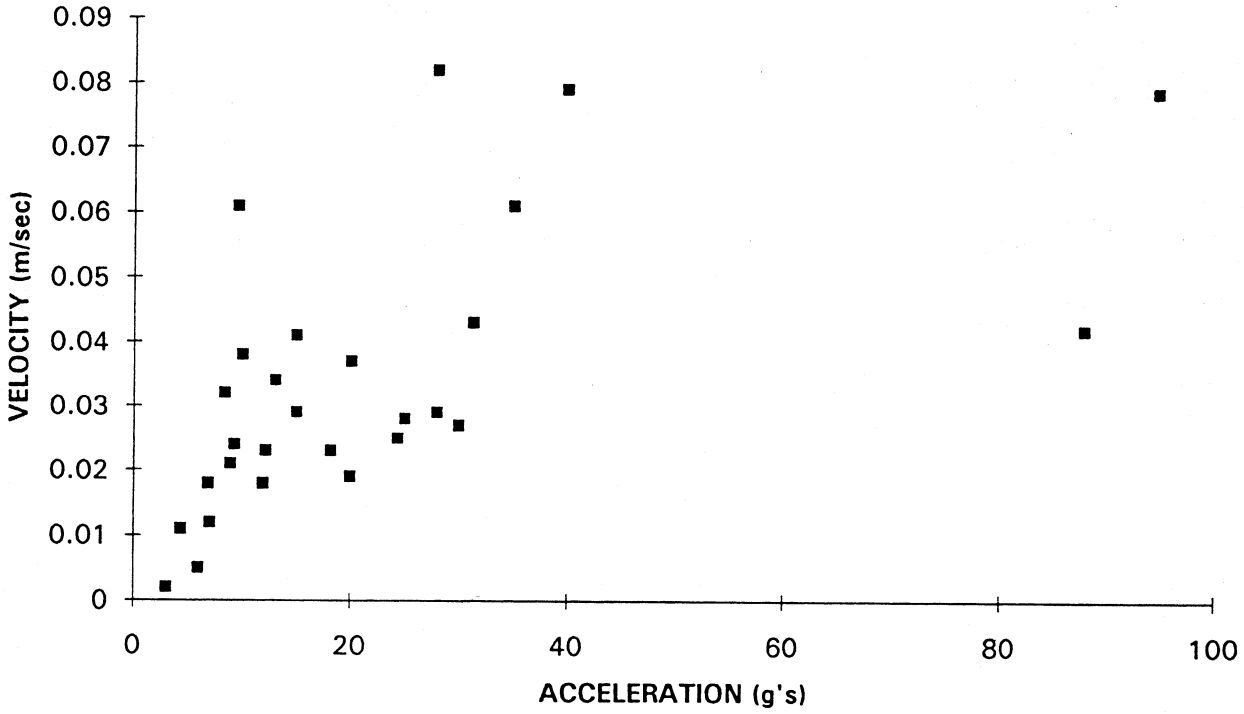

Figure 4. Plot of Impulse vs. Interface Stress

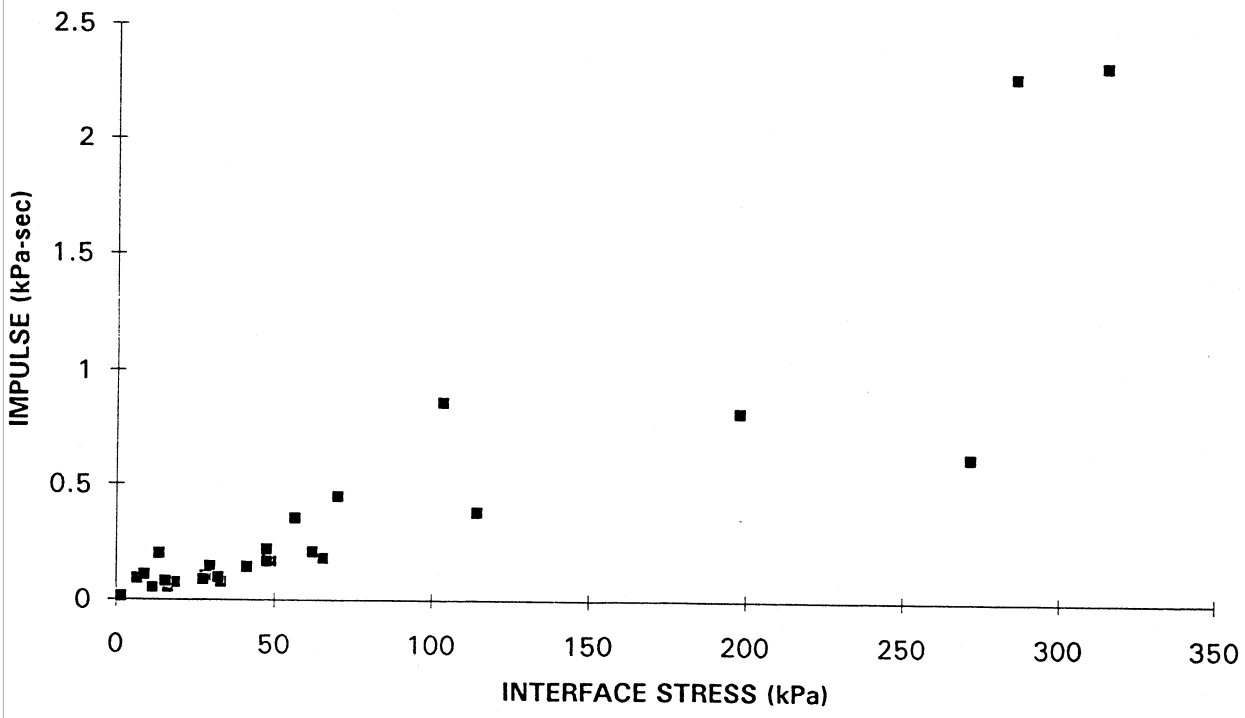

Figure 5. Plot of Velocity vs. Displacement

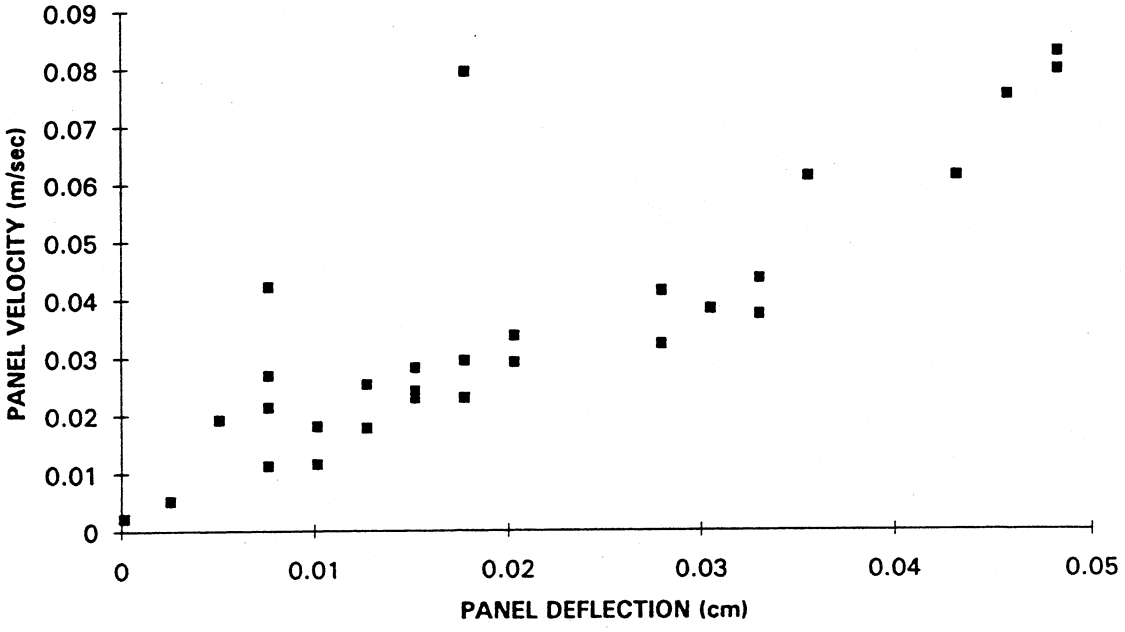

Pressure Versus Strain. Figure 6 shows the relationship between calculated pressure and strain in the respective geogrids for all tests. The pressure wave from the detonation of the explosive in the backfill outside of the reinforced soil zone caused the geogrid to go into compression. The data clearly shows, as expected, geogrid B required higher pressures to achieve the same level of compressive strain as geogrid A.

Figure 6. Plot of Free Field Pressure versus Geogrid Compressive Strain

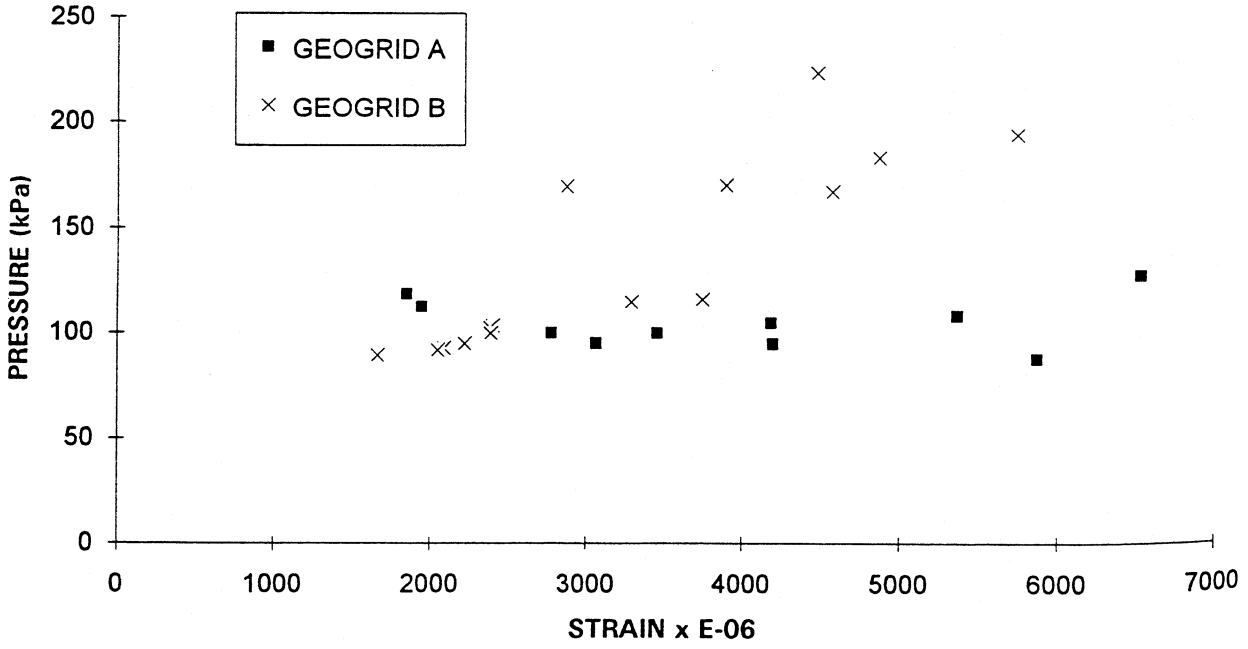

Displacements as a Function of Geogrid Type. Since the major wall deformations of the wall were caused by the formation of the explosive crater and not the detonation pressure wave, data was not obtained for the soil swell loads and their effect on the wall. However, posttest photographs qualitatively show the difference in wall response for geogrids A (fig 6) and B (fig 7) for a weapon standoff distance of 7.62m in the retained backfill, all other factors being equal.

FUTURE WORK

An equation of motion to determine the resistance of geogrid reinforced retaining walls and the accelerations and velocities of the wall panels is under development and will be published in the near future, as well as details of the strain gage installation procedure.

SUMMARY

This testing program provides some of the first detailed data on the pressures, accelerations and strains of a geogrid reinforced wall caused by a large underground explosion. Two mechanisms of loading were identified, the detonation pressure wave and the soil swell pressure generated during the formation of the explosive crater. The time differential between the arrival of these pressures are an order of magnitude apart. The test data quantifies the compressive strains in the geogrid during the passage of the pressure wave. Eighty percent of the accelerations caused by the detonation pressure wave were in the range of 3 to 30 g's, which qualifies the expected levels of acceleration and response for this type of loading. Also, this research has documented that the reinforced soil walls were extremely resistant to the high accelerations and pressures of the explosive generated pressure wave, and that this response was independent of the change in geogrid properties. However the walls are vulnerable to the soil swell. For the walls that failed, toe failures were observed. For the walls that did not fail, the pattern of wall displacement was strikingly similar to the measured results of the centrifuge tests. Qualitatively, increasing the geogrid stiffness greatly reduced the wall panel deflections caused by soil swell. Geogrid rupture or pullout were not observed in any of the tests. Finally, the static design methods used were appropriate for design against the pressure wave, however, for geogrid A (lower modulus), or for close in detonations, they were inadequate to resist the soil swell pressure.

ACKNOWLEDGEMENTS

The authors are would like to thank the U.S. Air Force Office of Scientific Research, Washington, DC, the Air Force Civil Engineering Laboratory, Tyndall Air Force Base, FL, and Tensar Earth Technologies, Inc., Atlanta, GA for their support in this research effort.

Figure 6. Posttest 3 - Geogrid A - Explosive at 7.62m

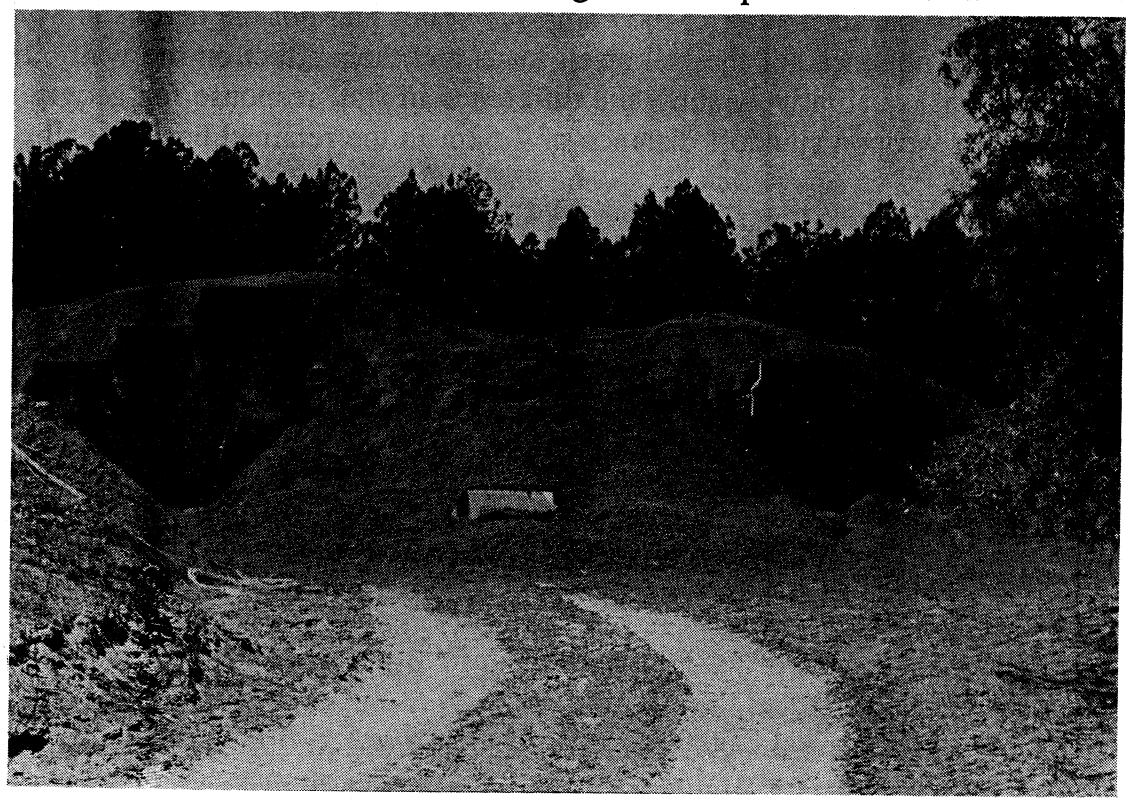

Figure 7. Posttest 5 - Geogrid B - Explosive at 7.62m

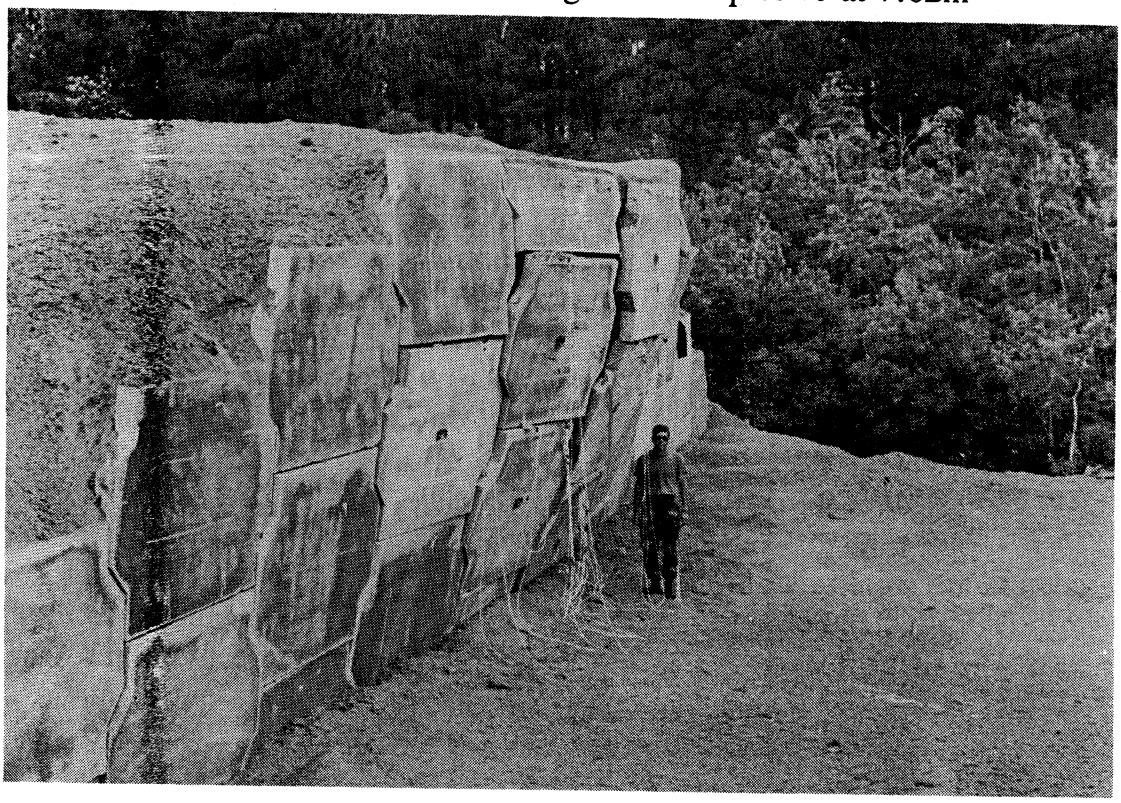

REFERENCES

Bachus, R.C., Fragaszy, R.J., Jaber, M., Olen, K.L., Yuan, Z., and Jewell, R., (1993) "Dynamic Response of Reinforced Soil Systems, Volume I and II", ESL-TR-92-47, Air Force Civil Engineering Support Agency, Tyndall Air Force Base, FL.

Christopher, B.R., Gill, S.A., Giroud, J.P., Juran, I., Mitchell, J.K., Schlosser, F., and Dunnicliff, J., (1990) "Reinforced Soil Structures: Volume I. Design and Construction Guidelines", FHWA-RD-89-043, United States Department of Transportation, McLean, VA.

Coltharp, D.R., Vitayaudom, K.P., and Kiger, S.A., (1985) "Semihardened Facility Design Criteria Improvement", ESL-TR-85-32, Air Force Engineering and Services Center, Tyndall Air Force Base, FL.

Drake, J.D. and Little, C.D., (1983) "Ground Shock from Penetrating Conventional Weapons", Symposium Proceedings form the Interaction of Non-Nuclear Munitions with Structures, U.S. Air Force Academy, Colorado, pp. 1-6.

Eytan, R. and Reid, R.A., (1993) "Reinforced Soil Ammunition Magazine: Full Scale Tests - 1990, Detailed Report ", (Confidential), Israel Air Force Civil Engineering Division, Tel Aviv, Israel, and U.S. Air Force Civil Engineering Support Agency, Tyndall AFB, FL.

Henrych, J., (1979) "The Dynamics of Explosion and Its Use", Elsevier Scientific Publishing Company, New York, New York.

Olen, K.L., Fragaszy, R.J., Purcell, M.R., and Cargill, K.W., (1994) "Dynamic Response of Reinforced Soil Systems: Phase II", draft report submitted to the U.S. Air Force Civil Engineering Laboratory, Tyndall Air Force Base, FL.

Olen, K.L., Fragaszy, R.J., Purcell, M.R., and Cargill, K.W., (1995) "Response of Reinforced Soil Walls to Explosive Loading: Part I - Centrifuge Modeling", Proceedings of Geosynthetics '95 Conference, IFAI, Nashville, TN.

Reid, R.A., (1995) "Conventional Weapons Effects in Reinforced Soil", Thesis presented to the Georgia Institute of Technology in partial fulfillment of the requirements for the degree of Doctor of Philosophy, Atlanta, GA.

Richardson, G.N., Feger, D., Fong, A., and Lee, K.L, (1977) "Seismic Testing of Reinforced Earth Walls", Journal of the Geotechnical Engineering Division, ASCE, Vol 103, No. GT1, pp. 1-17.

The Reinforced Earth Company Brochure, (undated) "Reinforced Earth ® Protective Structures For Industrial and Military Applications", McLean, VA.